iScience

CellPress
OPEN ACCESS

Article

Resident vascular Sca1^{+} progenitors differentiate into endothelial cells in vascular remodeling via miR-145-5p/ERG signaling pathway

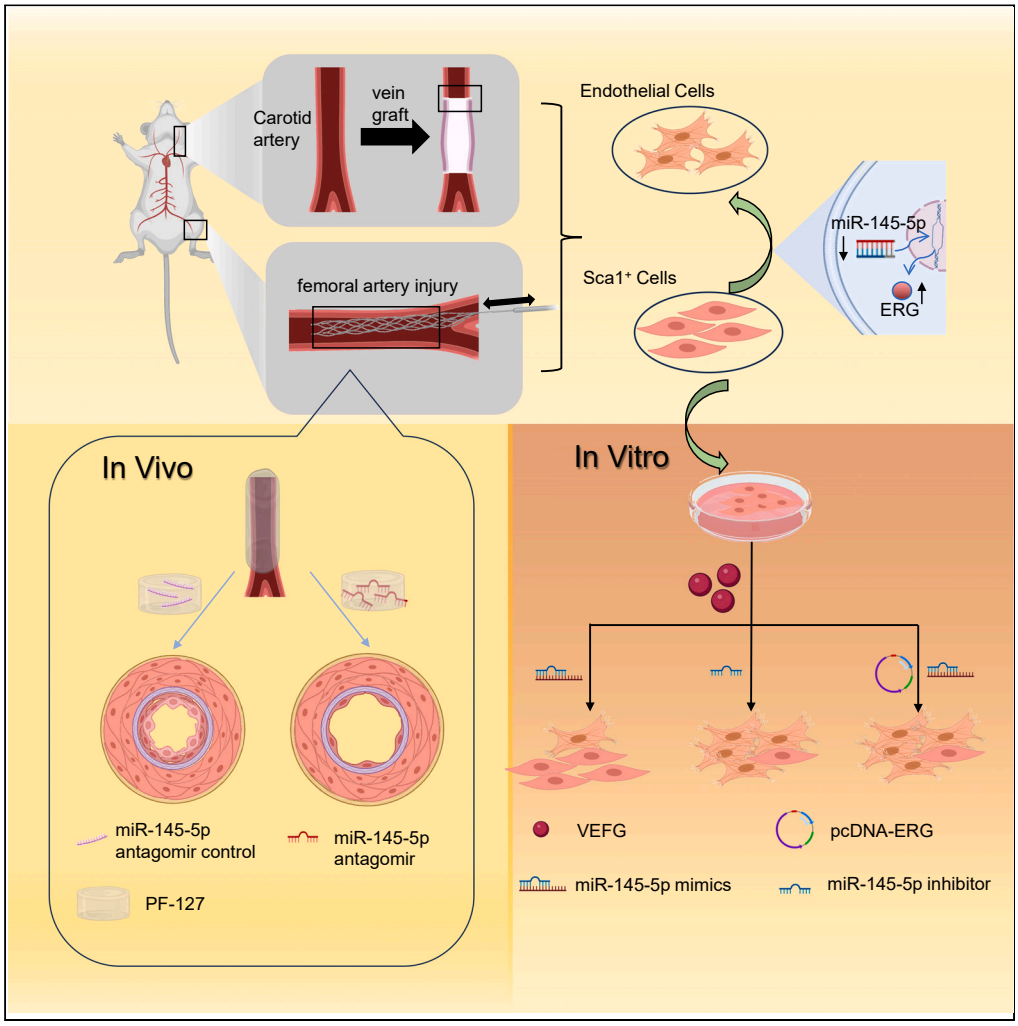

Zhangquan Ying, Lingxia Lyu, Xiaodong Xu, ..., Zhoubin Li, Liujun Jiang, Ting Chen

1510023@zju.edu.cn (Z.L.)
liujun_jiang@zju.edu.cn (L.J.)
ct010151452@zju.edu.cn (T.C.)

Highlights

Sca1^{+} progenitors are able to differentiate into ECs, both *in vivo* and *in vitro*

Negative regulation of miR-145-5p/ERG pathway is key to Sca1^{+} cells' differentiation

Inhibiting miR-145-5p in Sca1^{+} cells repairs ECs and reduces vascular remodeling

Ying et al., iScience 27, 110080
June 21, 2024
https://doi.org/10.1016/j.isci.2024.110080

iScience

CellPress
OPEN ACCESS

Article

Resident vascular Sca1$^+$ progenitors differentiate into endothelial cells in vascular remodeling via miR-145-5p/ERG signaling pathway

Zhangquan Ying,[1,4] Lingxia Lyu,[1,4] Xiaodong Xu,[1] Zuoshi Wen,[1] Jianing Xue,[1] Mengjia Chen,[1] Zhoubin Li,[2,*] Liujun Jiang,[1,*] and Ting Chen[1,3,5,*]

SUMMARY

Endothelial cell (EC) damage or dysfunction serves as the initial event in the pathogenesis of various cardiovascular diseases. Progenitor cells have been postulated to be able to differentiate into ECs, facilitate endothelial regeneration, and alleviate vascular pathological remodeling. However, the precise cellular origins and underlying mechanisms remain elusive. Through single-cell RNA sequencing (scRNA-seq), we identified an increasing population of progenitors expressing stem cell antigen 1 (Sca1) during vascular remodeling in mice. Using both mouse femoral artery injury and vein graft models, we determined that Sca1$^+$ cells differentiate into ECs, restored endothelium in arterial and venous remodeling processes. Notably, we have observed that the differentiation of Sca1$^+$ cells into ECs is negatively regulated by the microRNA-145-5p (miR-145-5p)-Erythroblast transformation-specific-related gene (ERG) pathway. Inhibiting miR-145-5p promoted Sca1$^+$ cell differentiation and reduced neointimal formation after vascular injury. Finally, a similar downregulation of miR-145-5p in human arteriovenous fistula was observed comparing to healthy veins.

INTRODUCTION

Endothelial cells (ECs) form the lining of the inner walls of blood and lymph vessels. The renewal, repair, and regeneration of these vascular ECs are essential for maintaining tissue homeostasis and are also crucial in the development of various vascular diseases, including atherosclerosis, restenosis following angioplasty, and venous remodeling.[1,2] After endothelial damage or denudation in large arteries, regeneration of ECs is usually one of the most critical steps in lesion healing. Studies on the regeneration of ECs have identified many types of endothelial progenitor cells, such as embryonic stem cells,[3,4] induced pluripotent stem cells,[5–7] vascular progenitor cells,[8,9] or terminally differentiated cell lines.[10]

Recent studies identified the presence of multiple endothelial progenitor cells in the vessel wall, and they express CD34,[11,12] stem cell factor receptor (c-Kit),[13] fetal liver kinase-1 (Flk-1),[14] and stem cells antigen 1 (Sca1).[12] Sca1, also named lymphocyte antigen 6 complex locus A (*Ly6a*), belongs to the ly-6 family and is recognized as a cell surface marker for hematopoietic stem cells.[15] Tang et al.[16] conducted a study using a Sca1 lineage tracing transgenic mouse model to propose that vascular Sca1$^+$ progenitor cells adopt the EC fate during the injury and repair process of large arteries. Adult Sca1$^+$ cells isolated from myocardium are able to differentiate into ECs.[17] However, further investigation is required to understand the mechanisms underlying the participation of Sca1$^+$ cells in vascular remodeling and the transition of Sca1$^+$ progenitors to ECs, as this process remains poorly understood.

In this study, we employed single-cell RNA sequencing (scRNA-seq) analyses and a Sca1-CreER^{T2};Rosa26-tdTomato lineage tracing mouse model, combing with femoral artery guidewire injury and vein graft surgeries, to investigate the acquisition of EC fate by Sca1$^+$ cells during arterial and venous remodeling, both *in vivo* and *in vitro*. *In vitro* experiments demonstrated that the differentiation of Sca1$^+$ cells into ECs was regulated by the miR-145-5p/ERG pathway. Inhibition of miR-145-5p reduced neointimal hyperplasia and enhanced the EC differentiation of Sca1$^+$ cells *in vivo*. Similar reduced expression of miR-145-5p was examined in human arteriovenous fistula (AVF) samples comparing to healthy veins. These findings provide compelling evidence that Sca1$^+$ cells can differentiate into ECs during vascular repair, with miR-145-5p serving as an important regulator in multiple vascular diseases.

[1]Department of Cardiology, the First Affiliated Hospital, Zhejiang University School of Medicine, Hangzhou 310003, China
[2]Department of Lung Transplantation and General Thoracic Surgery, The First Affiliated Hospital, Zhejiang University School of Medicine, Hangzhou 310003, China
[3]Key Laboratory of Precision Medicine for Atherosclerotic Diseases of Zhejiang Province, Affiliated First Hospital of Ningbo University, Ningbo 315010, China
[4]These authors contributed equally
[5]Lead contact
*Correspondence: 1510023@zju.edu.cn (Z.L.), liujun_jiang@zju.edu.cn (L.J.), ct010151452@zju.edu.cn (T.C.)
https://doi.org/10.1016/j.isci.2024.110080

RESULTS

scRNA-seq analyses revealed that Sca1$^+$ cells repopulate ECs in mouse femoral artery injury

To elucidate the functional role of Sca1$^+$ cells in arterial intima injury and repair, we obtained single-cell transcriptomic data from GEO's database for injured mouse femoral arteries (GSE182232).[11] The endothelium was denuded using femoral artery guidewire injury surgery. Following this procedure, ECs underwent regeneration to repair the endothelium and facilitate neointima lesion formation. The dataset includes samples from normal femoral arteries (NC) and those injured for 2 (FAI2W) or 4 (FAI4W) weeks. Post-quality control, we obtained 6760, 7084, and 8184 cells from each of these groups. We identified twenty cell clusters through unsupervised clustering with Umap embedded in Seurat analysis (Figure S1A). Based on the highest gene expression levels (Figure S1B) and canonical cell type markers (Figure S1C), we assigned presumptive biological identities to each cluster (Figure 1A). The dot plot analysis indicated that *Pecam1*, *Cdh5*, *Flt1*, *Kdr*, and *Nos3* were exclusive to the EC population, whereas the *Pdgfra* mesenchymal marker predominantly appeared in mesenchymal populations. A cluster expressing high levels of *Cd34* and *Ly6a* (encoding Sca1) was designated as stem/progenitor cells (SPCs). Noteworthy, both SPCs and ECs exhibited high expression of *Ly6a* (Figure 1B).

ECs were further segregated into *Ly6a*-positive (*Ly6a*$^+$) and *Ly6a*-negative (*Ly6a*$^-$) subpopulations, and it was observed that the *Ly6a*$^+$ ECs exhibited a significant increase post-injury, as illustrated in Figure 1C. Subsequently, a gene ontology (GO) analysis of the differentially expressed genes between the *Ly6a*$^+$ and *Ly6a*$^-$ ECs revealed an enrichment of biological process terms associated with the regulation of angiogenesis, vascular development, and epithelial cell proliferation (Figure 1D). For trajectory analysis, specific clusters of ECs and Sca1$^+$ progenitor cells (SPCs) were identified. Figure 1E delineated a more primitive developmental state of SPCs (green) compared to ECs (blue). In the FAI2W group, a considerable number of cells were observed transitioning between SPCs and ECs, suggesting an active reparative process post-injury. The pseudotime trajectory analysis also revealed a downregulation in the expression of *Ly6a*, *Cd34*, and *Pdgfra* and an upregulation in *Cdh5*, *Flt1*, *Nos3*, and *Pecam1* as cells progressed from SPCs (orange) to ECs (green) (Figure 1F). These findings suggested that Sca1$^+$ cells could potentially differentiate into ECs to facilitate endothelial restoration during vascular repair.

Vascular Sca1$^+$ cells exhibit endothelial differentiation potential in both arterial and venous remodeling *in vivo*

To further explore the function of Sca1$^+$ cells *in vivo*, we utilized Sca1 lineage tracing mice (Sca1-CreER^{T2}; Rosa26-tdTomato). Our initial investigations focused on arterial disease through performing guide wire injury surgeries on the femoral arteries of mice. In healthy femoral arteries (Figure 2A), tdTomato-labeled Sca1$^+$ cells were scarcely present in the endothelium, with tdTomato$^+$ CD31$^+$ cells comprising only a small fraction of the EC population. Predominantly, tdTomato$^+$ CD31$^-$ cells were found in the arterial adventitia. Four weeks post-surgery, the injured femoral arteries exhibited a marked increase in tdTomato$^+$ CD31$^+$ ECs within the intima, as shown in Figure 2B. Quantitative analysis revealed a significant rise in the proportion of tdTomato$^+$ ECs post-injury, escalating from 11.90 $\pm$ 7.16% in healthy specimens to 33.43 $\pm$ 6.36% in injured ones (Figure 2C). Additionally, immunofluorescent staining of injured femoral arteries revealed the co-expression of Sca1 and CD31 in cells within the vascular wall (Figure S2), suggesting the *in vivo* differentiation of Sca1$^+$ cells into CD31$^+$ cells.

Subsequently, we examined the influence of Sca1$^+$ cells on venous remodeling by conducting vein graft experiments. In vein graft models, inferior vena cava of the mouse was transplanted and connected to the carotid artery, which were subject to a more intense vascular remodeling process. During vein grafting, ECs are not immediately harmed but gradually sustain damage due to enhanced blood flow and elevated shear stress. In the vena cava, tdTomato$^+$ CD31$^+$ ECs constituted a small portion of the endothelial population (Figure 3A). At four weeks post-operation, endothelial lining of vein grafts showed a progressive replacement of tdTomato$^-$ CD31$^+$ ECs with tdTomato$^+$ CD31$^+$ ECs. These cells were also observed in the adventitial vasa vasorum (Figure 3B). Quantitative analysis revealed a rise in the percentage of tdTomato$^+$ ECs after venous remodeling, increasing from 11.90 $\pm$ 5.01% in the vena cava to 39.14 $\pm$ 7.41% in vein grafts (Figure 3C). Collectively, these data suggested that Sca1$^+$ cells were capable of differentiating into ECs *in vivo*.

To further examine the necessity of Sca1$^+$ cells in the vascular remodeling of vein grafts, Sca1-CreER^{T2}; Rosa26-tdTomato mice were bred with Rosa26-iDTR mice. Selective ablation of Sca1$^+$ cells was achieved by inducing the expression of diphtheria toxin receptors (DTR) in these cells through tamoxifen administration. Subsequent introduction of diphtheria toxin (DT) led to the apoptotic elimination of the targeted Sca1$^+$ cells. The targeted depletion of Sca1$^+$ cells resulted in a significant reduction in tdTomato$^+$ CD31$^+$ EC regeneration (Figure 3D), which may further affect neointimal formation and venous remodeling in the long-term.

Isolated Sca1$^+$ cells differentiated into ECs with VEGF treatment *in vitro*

Subsequent investigations were aimed at ascertaining the capacity of isolated Sca1$^+$ cells differentiating into ECs *in vitro*. Primary mouse aortic adventitial Sca1$^+$ cells were propagated in EGM-2 medium fortified with Vascular Endothelial Growth Factor (VEGF). Over the course of the first five days of culture, a morphological transition of the cells from spindle-shaped to tube-like structures was observed (Figure 4A), with the formation of rudimentary tubes appearing by day 3. By day 5, the cells exhibited increased connectivity, and the tubes presented with enhanced width and thickness. Concurrently, there was a marked upregulation of endothelial-specific genes, including *Kdr*, *Flt1*, *and Pecam1* (Figure 4B). Investigations into protein expression revealed an initially low presence of endothelial-specific proteins such as PECAM1, CDH5, and KDR in Sca1$^+$ cells; however, their levels surged following exposure to EGM-2 and VEGF (Figures 4C and 4D). Immunofluorescent staining disclosed that Sca1$^+$ cells, initially dispersed across the culture plate, began to aggregate and form tubular structures post-treatment, coinciding with a substantial increase in CD31 (PECAM1) expression (Figure 4E). These results substantiated the *in vitro* differentiation prowess of vascular Sca1$^+$ cells into ECs.

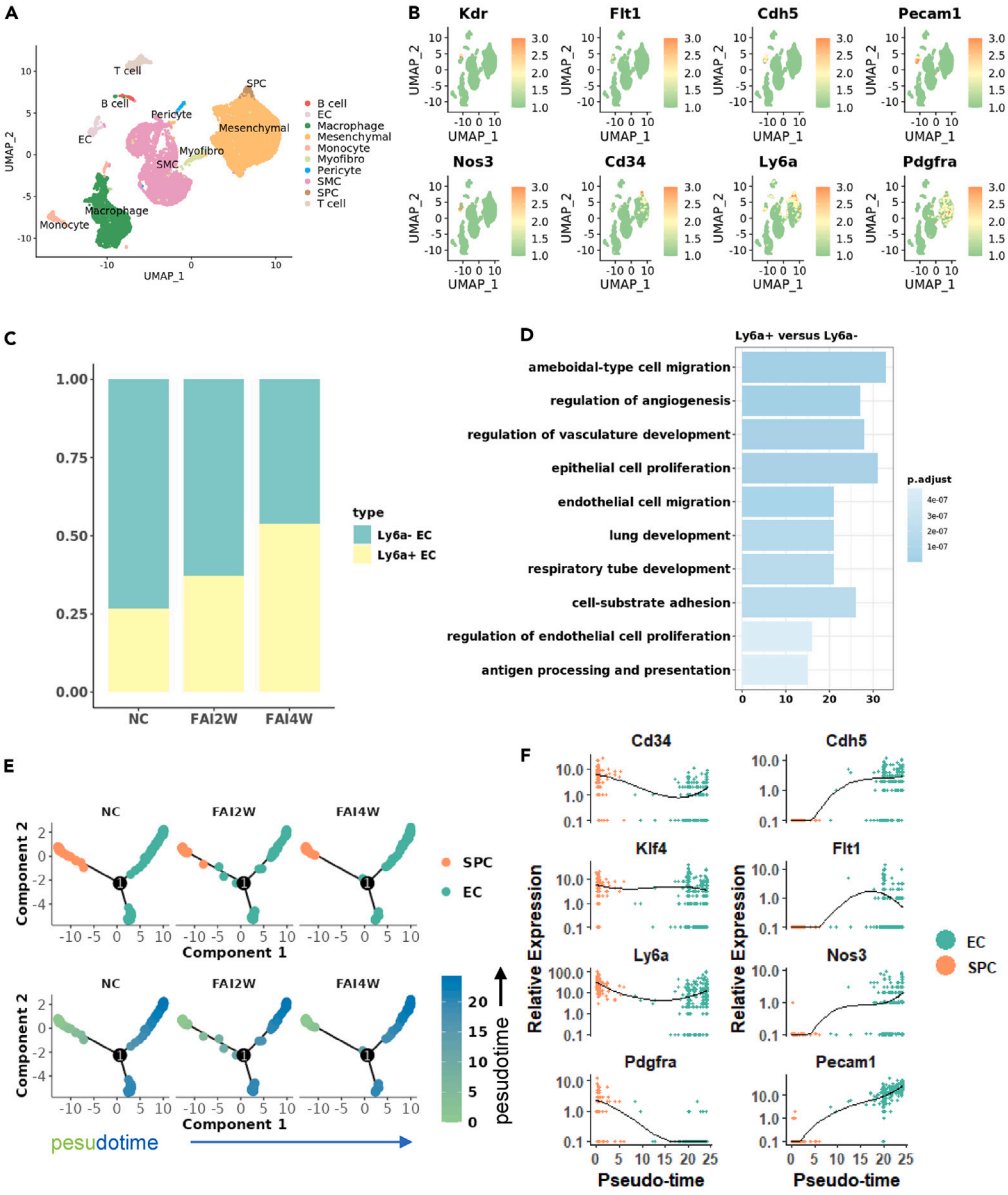

Figure 1. scRNA-seq analyses revealed Sca1$^+$ cells repopulate ECs in mouse femoral artery after injury

(A) Normal femoral arteries (NC) and injured femoral arteries were digested and analyzed by scRNA-seq after 2 (FAI2W) or 4 (FAI4W) weeks. Umap plot showed visualization of unsupervised clustering of all groups.

(B) Dot plot of canonical cell markers identified EC cluster (*Kdr*, *Flt1*, *Cdh5*, *Pecam1*, and *Nos3*) and SPC cluster (*Cd34*, *Ly6a*, and *Pdgfra*).

(C) Bar plot showed the constitution of *Ly6a* (Sca1)$^+$ or *Ly6a*$^-$ cells among ECs of each group.

(D) Differentially expressed genes between *Ly6a*$^+$ and *Ly6a*$^-$ cells were identified and analyzed using GO enrichment. The top 10 enriched biological process terms were presented.

(E) Trajectory analysis of the differentiation process from SPCs to ECs; the color change from green to blue indicates the cell's progression from a primitive to a more developed state.

(F) The expression levels of canonical EC markers and SPC markers are shown alongside the differentiation trajectory. See also Figure S1.

MiR-145-5p regulated Sca1$^+$ cell differentiating into ECs

We next sought to explore the mechanism underlying Sca1$^+$ cells differentiating into ECs. Previous studies have reported that miR143/145 and miR199a/199b[18] play important roles in endothelial regeneration. Therefore, we investigated the expression patterns of certain microRNAs during Sca1$^+$ cell differentiation. Transient downregulation was observed for miR-143, miR-199a, and miR-199b-5p (Figure S3A), and modulation of these microRNAs' levels was found to influence the differentiation process to a certain degree (Figure S3B). Notably,

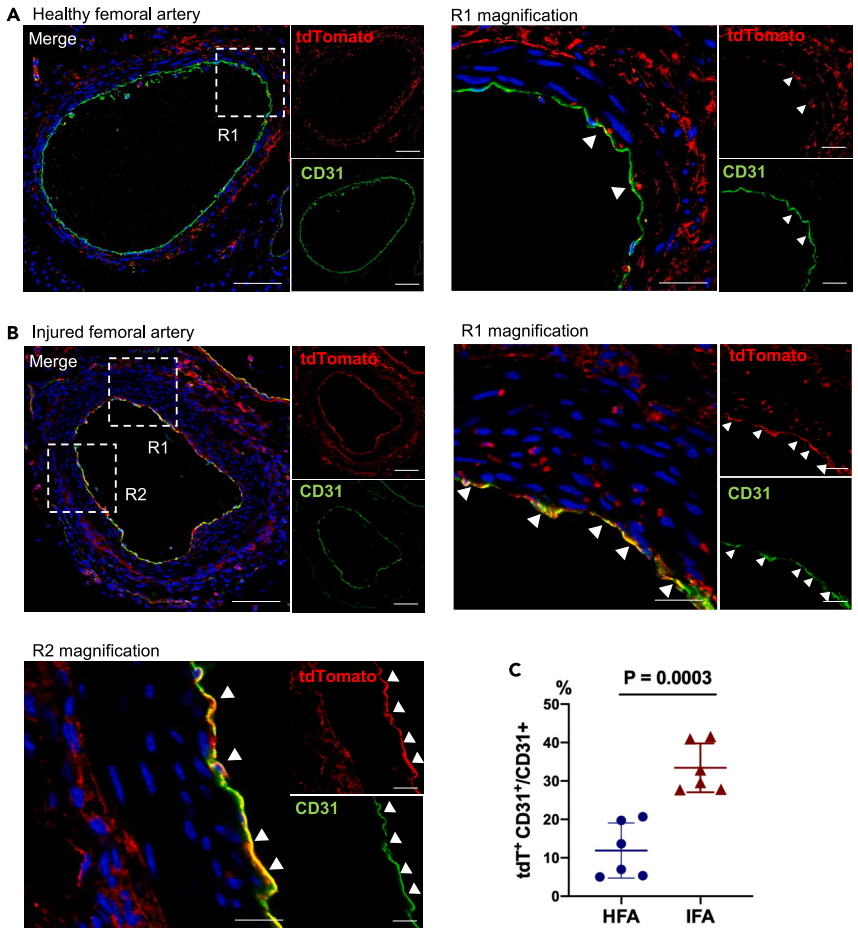

Figure 2. Vascular Sca1$^+$ cells exhibit endothelial differentiation potential in artery injury and repair

(A) Immunofluorescence staining of healthy femoral artery for CD31 and Sca1$^+$ lineage marker tdTomato (tdT) using Sca1-CreER^{T2};Rosa26-tdTomato mouse model. The right panel showed magnification of the boxed region.

(B) Immunofluorescence staining of injured femoral artery for CD31 and tdTomato (Sca1$^+$ lineage). The right panel and the panel below showed magnification of the boxed regions. For merge images, scale bars, 100 μm. For magnification images, scale bars, 20 μm.

(C) Quantification of the percentage of CD31$^+$ tdT$^+$ cells in CD31$^+$ cells of healthy femoral artery (HFA) and injured femoral artery (IFA). Data represent mean ± SEM, $n = 6$ in each group. p value was specified in the graph. Statistical differences between groups were determined by two-tailed Student's t test for normally distributed values. See also Figure S2.

miR-145-5p expression consistently exhibited significant reduction throughout the differentiation progression (Figures 5A and 5B). Furthermore, we examined the impact of miR-145-5p manipulation on the expression of endothelial markers in Sca1$^+$ cells treated with VEGF. Overexpression of a miR-145-5p mimic led to a decline in canonical endothelial markers, such as *Pecam1*, *Flt*, and *Cdh5* (Figure 5C), whereas inhibition of miR-145-5p produced the contrary effect (Figure 5D). Western blot analyses corroborated these findings, showing that miR-145-5p overexpression reduced protein levels of PECAM1, CDH5, and KDR, while its suppression elevated PECAM1 and KDR levels (Figure 5E and 5F). In alignment with these results, immunofluorescence staining demonstrated that miR-145-5p overexpression reduced CD31 protein expression (Figure 5G and 5H).

Effects of miR-145-5p on the proliferation and migration of Sca1$^+$ cells

Despite the differentiation process, previous studies have shown that miR-145-5p can affect the proliferation and migration of vascular smooth muscle cells.[19] However, the impact of miR-145-5p on Sca1$^+$ cell activity remains to be elucidated. To address this, we conducted a CCK-8 assay, which revealed no significant difference in proliferation between the miR-145-5p mimic group and the control group (Figure 6A). Additionally, the transwell migration assay indicated that miR-145-5p mimic transfection diminished the migration capacity of Sca1$^+$ cells (Figure 6B). The wound healing assay results corroborated this finding, as the area of wound closure in the miR-145-5p mimic group was reduced (Figure 6C). Collectively, our findings suggested that miR-145-5p overexpression inhibits the migration of adventitial Sca1$^+$ cells and their subsequent differentiation into ECs.

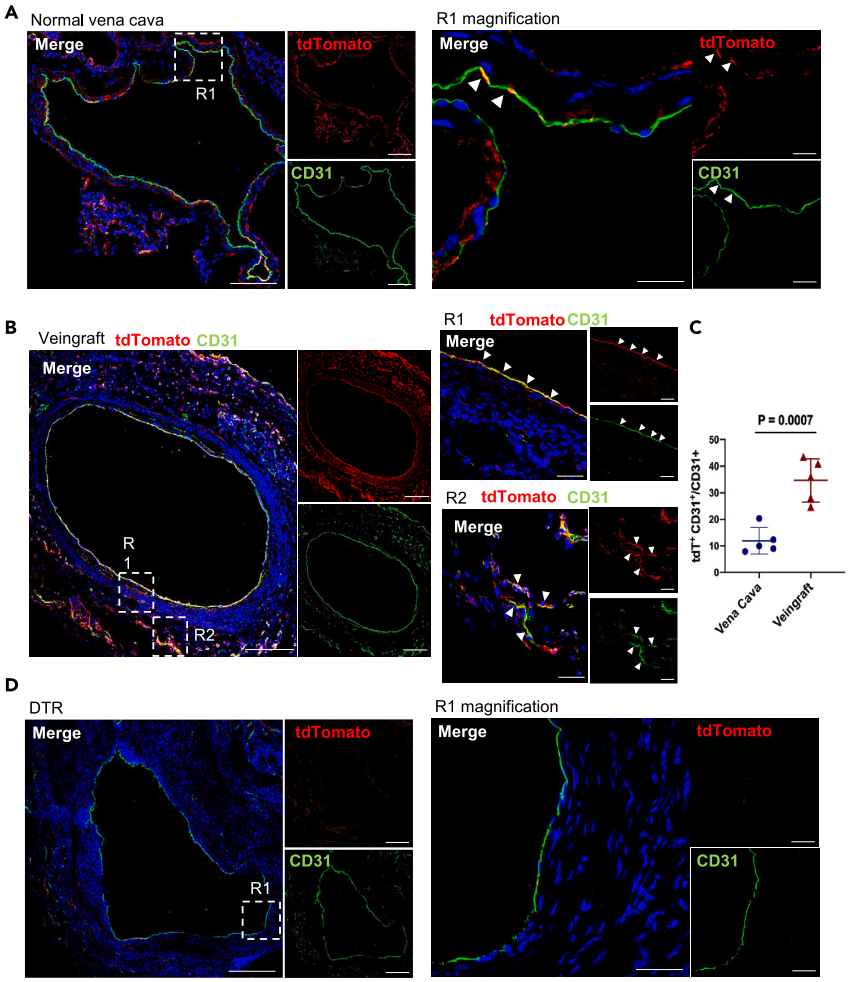

Figure 3. Vascular Sca1$^+$ cells differentiate into ECs in vein graft

(A) Immunofluorescence staining of normal vena cava for CD31 and tdTomato (tdT, Sca1$^+$ lineage). The right panel showed magnification of the boxed region.

(B) Immunofluorescence staining of vein graft for CD31 and tdTomato. The right panel and the panel below showed magnification of the boxed regions.

(C) Quantification of the percentage of CD31$^+$ tdT$^+$ cells in CD31$^+$ cells of both groups.

(D) Sca1-CreER^{T2}; Rosa26-tdTomato mice were bred with Rosa26-iDTR mice. Tamoxifen was given to label Sca1$^+$ cells and diphtheria toxin (DT) injection was performed to ablate certain cells. Immunostaining for tdTomato and CD31 on vein graft sections after DT administration. For merge images, scale bars, 100 μm. For magnification images, scale bars, 20 μm. Data represent mean ± SEM, n = 5 in each group. p value was specified in the graph. Statistical differences between groups were determined by two-tailed Student's t test for normally distributed values.

MiR-145-5p regulates the differentiation of Sca1$^+$ cells into ECs by targeting ERG

We further examined the role of miR-145-5p in directing the differentiation of Sca1$^+$ cells into ECs. Utilizing the TargetScan database, we found that miR-145-5p is capable of targeting the 3′-untranslated region (3′UTR) of the mRNA for Erythroblast transformation-specific-related gene (ERG) (Figure 7A). ERG, a critical transcription factor, orchestrates the development of ECs.[20] We first detected Sca1$^+$ ERG$^+$ cells in femoral guidewire injury (Figures S4A, and S4B) and veingraft models (Figures S4C, and S4D), and found significant increases of Sca1$^+$ ERG$^+$ cells in diseased conditions. Consequently, we postulated that miR-145-5p regulates Sca1$^+$ cell differentiation by targeting ERG. Dual-luciferase reporter gene assays using ERG-3′UTR reporter constructs were used to confirm the interaction between miR-145-5p and ERG (Figure 7B), while no impact was observed with the mutant construct (Figure 7C). RT-PCR verified that miR-145-5p mimic promoted the degradation of *Erg* mRNA in Sca1$^+$ cells (Figure 7D). Overexpression of ERG promoted Sca1$^+$ cells differentiating into ECs with upregulation of canonical EC markers in both mRNA and protein levels (Figures 7E–7G). Subsequent experiments indicated that ERG overexpression strengthened Sca1$^+$ cell differentiation into ECs, a process initially inhibited by miR-145-5p mimics, through the increased expression of specific EC markers at the mRNA and protein levels (Figures 7H–7J). Immunofluorescence analyses also exhibited that miR-145-5p mimic markedly reduced CD31 and ERG expression in Sca1$^+$ cells under VEGF stimulation, while miR-145-5p inhibitor markedly increased their expression (Figures S5A, and S5B). Collectively, these findings indicated that miR-145-5p inhibited the differentiation of Sca1$^+$ cells into ECs by targeting ERG.

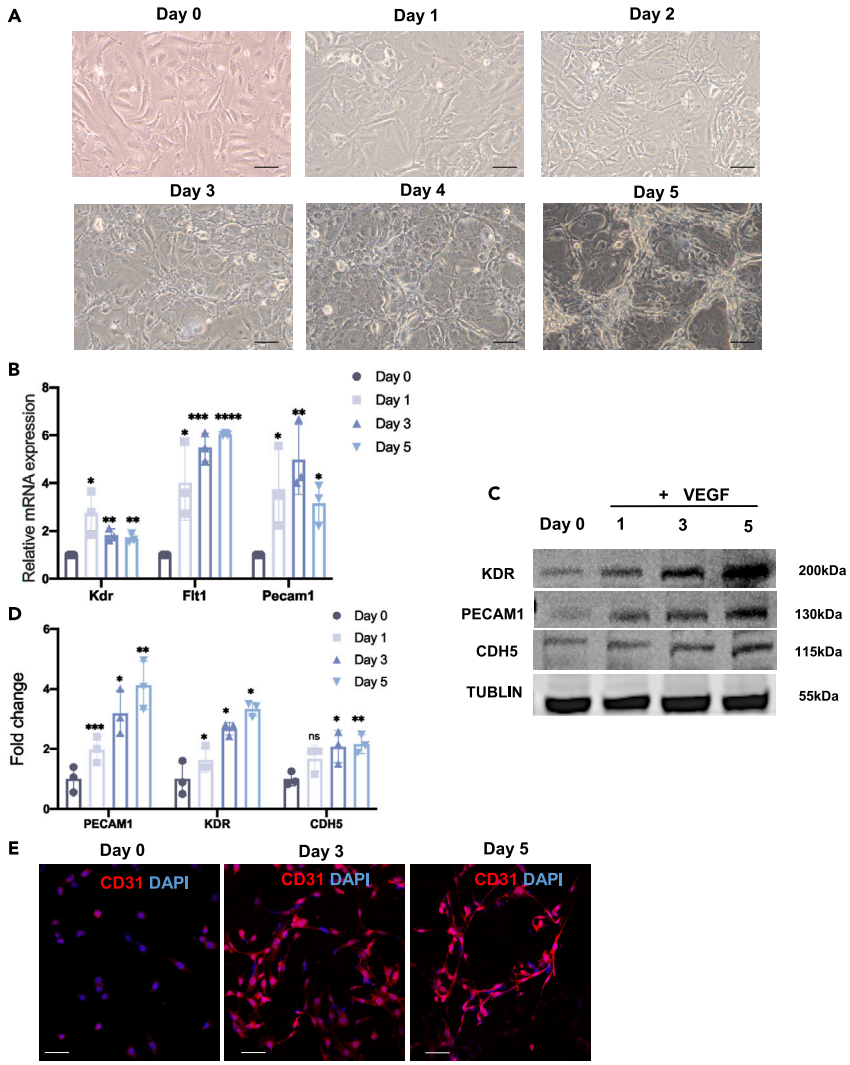

Figure 4. Isolated Sca1$^+$ cells could differentiate into ECs with VEGF treatment *in vitro*

(A) The morphological changes in Sca1$^+$ cells after treatment with 50 ng/ml VEGF for 0–5 days.

(B) mRNA expression level of EC markers *Kdr*, *Flt1*, and *Pecam1* as determined by RT-PCR at different time points after culture with VEGF.

(C) Protein expression level of PECAM1, CDH5, and KDR as determined by western blotting assay.

(D) Protein bands were quantified by densitometry and normalized to the density of Tubulin.

(E) Immunofluorescence staining of CD31 in Sca1$^+$cells treated with VEGF at different time points. Scale bars, 25 μm. Data represent mean ± SEM. ***$p < 0.001$, **$p < 0.01$, ns $p \geq 0.05$. $n = 3$ in each group. Statistical differences between groups were determined by one-way ANOVA analysis of variance with method of multiple comparisons.

To further examine the therapeutic potential of miR-145-5p in postinjury arterial remodeling, 2.5 nmol of miR-145-5p loss-of-function antagomiR or antago-control was perivascularly applied to femoral arteries immediately after guidewire injury on Sca1-CreER^{T2}; Rosa26-tdTomato mice and it was found that miR-145-5p inhibition reduced post-injury neointimal formation (Figures S6A, and S6B). Increased tdTomato$^+$ CD31$^+$ ECs were also observed, indicating an enhanced Sca1$^+$ cell differentiation into ECs, with an increase of ERG expression in them (Figure S6C). We also collected samples from normal human cephalic veins and arteriovenous fistulas (AVFs) to investigate the role of the miR-145-5p/ERG pathway in human venous remodeling. As humans do not express the Sca1 marker, we assessed the well-established progenitor cell marker CD34. Our findings revealed a significant increase in CD34$^+$ ERG$^+$ cells in AVFs when compared to normal cephalic veins (Figure S7). Furthermore, miR-145-5p expression was found to be reduced in AVFs relative to that in normal veins (Figure 7K). These observations imply that a reduction in miR-145-5p may facilitate the differentiation of CD34$^+$ progenitor cells into ECs by targeting ERG during venous remodeling in humans. In fistulas, ECs are damaged by augmented blood flow and shear stress, and their regeneration plays a critical role in neointima formation. The decreased expression of miR-145-5p may be associated with excessive EC regeneration from progenitor cells, potentially contributing to neointima hyperplasia. Consequently, miR-145-5p could serve as a predictive biomarker for the diagnosis and prognosis of human vascular diseases.

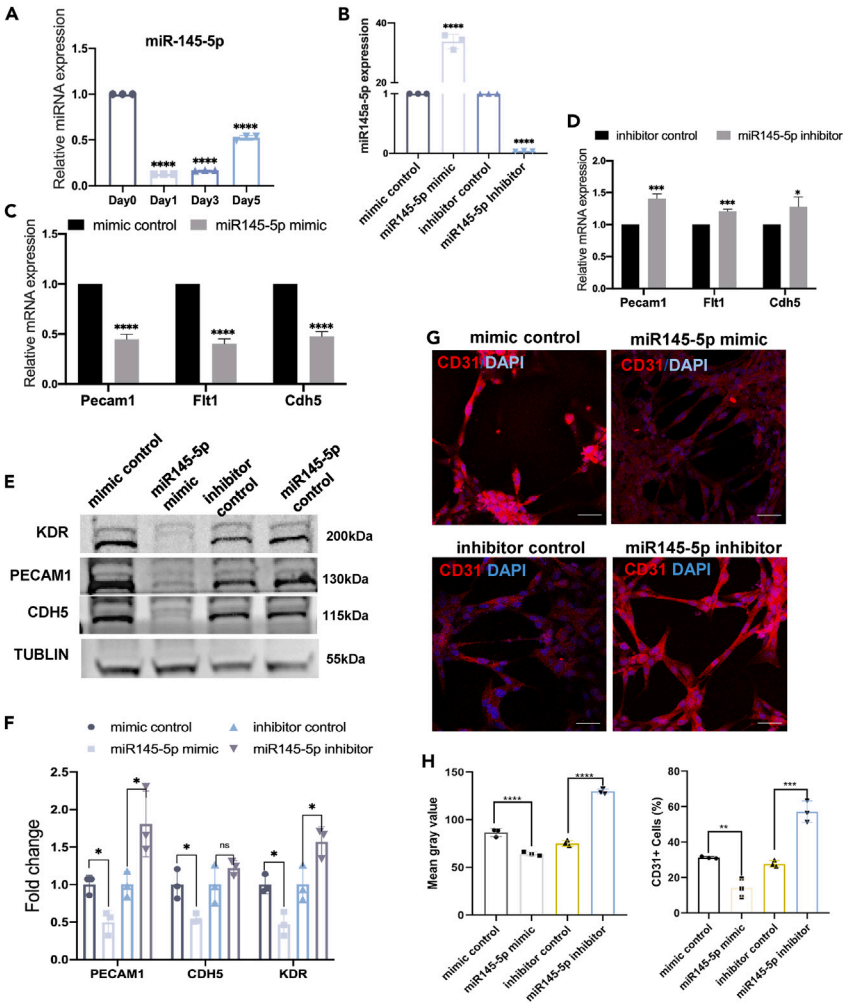

Figure 5. The effect of miR-145-5p on the differentiation of Sca1$^+$ cells to ECs with VEGF treatment

(A) RT-PCR analysis for the expression of miR-145-5p in Sca1$^+$ cells treated with VEGF at different time points.

(B) RT-PCR showed expression of miR-145-5p in Sca1$^+$ cells after transfection with mimic control/miR-145-5p mimic and inhibitor control/miR-145-5p inhibitor.

(C) and (D) RT-PCR analysis for the expression of *Pecam1*, *Flt1*, and *Cdh5* in Sca1$^+$ cells transfected with mimic control/miR-145 mimic or inhibitor control/miR-145 inhibitor and cultured in VEGF.

(E) the protein expression level of PECAM1, CDH5 and KDR as determined by western blotting assay in each group.

(F) Protein bands were quantified by densitometry and normalized to the density of Tubulin.

(G) Immunofluorescence staining of CD31 (*Pecam1*) in Sca1$^+$ cells and (H) analysis for fluorescence intensity of CD31 in each group, $n = 3$. scale bars, 25 μm. Data represent mean ± SEM. $^{**}p < 0.01$, $^{***}p < 0.001$, ns $p \geq 0.05$. Statistical differences between groups were determined by one-way analysis of variance with method of multiple comparisons. See also Figure S3.

DISCUSSION

Endothelial injury and subsequent repair constitute a crucial initial phase in the pathogenesis of vascular diseases, including atherosclerosis, angioplasty-induced vessel injuries, and in-stent restenosis.[21] The isolation of putative endothelial progenitor cells (EPCs) from peripheral blood mononuclear cells has given rise to progenitor cell therapy,[22] which has been explored extensively in clinical trials for the treatment of cardiovascular diseases. Nevertheless, the highly variable outcomes of these trials have significantly impeded the therapy's translation into clinical practice.[23–25] Recent studies have identified tissue-resident Sca1$^+$ cells within the vessel wall.[26–28] However, their exact origin and function in endothelial regeneration are yet to be elucidated. The current study has established that vascular Sca1$^+$ progenitor cells can differentiate into ECs both *in vivo* and *in vitro*, a process essential for vascular injury repair. Over the last 20 years, a substantial body of research has suggested that Sca1$^+$ progenitor cells from various sources are capable of giving rise to ECs. Furthermore, it has been shown that Sca1$^+$ stem cells originating from skeletal muscle can undergo differentiation into ECs, thereby enhancing the efficacy of muscle regeneration.[29] Mature myocardium-derived Sca1$^+$ cells have also been reported to undergo differentiation into ECs.[29–31] These results imply that Sca1 could serve as a biomarker for endothelial progenitor cells. While various stem cells or fully differentiated cell lines have the capability to

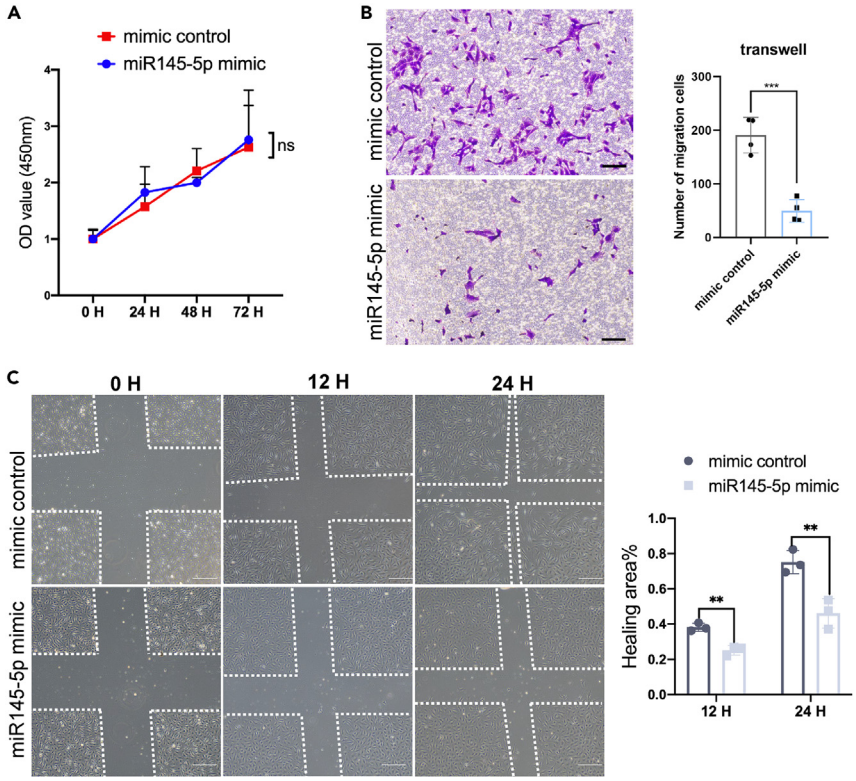

Figure 6. The effects of miR-145-5p on the proliferation and migration of Sca1$^+$ cells

(A) CCK8 assay for the effect of miR-145-5p overexpression on the proliferation of Sca1$^+$ cells. Transwell migration assay (B) and wound healing assay (C) for the effect of miR-145-5p overexpression on the migration of Sca1$^+$ cells. $n = 3$ in each group. Scale bars, 25 μm. Data represent mean ± SEM. *$p < 0.05$, **$p < 0.01$, ns $p \geq 0.05$. Statistical differences between groups were determined by two-tailed Student's t test for normally distributed values.

produce ECs via a complex array of factors, the intricacy of these protocols and their modest efficiencies present substantial barriers to clinical implementation. In this study, we extracted Sca1$^+$ cells from the mouse aorta and prompted their differentiation into ECs over a brief period using recombinant VEGF, which is a quick, straightforward, and ethically sound approach.

MicroRNAs (miRNAs) are small endogenous non-coding RNA molecules, approximately 21–25 nucleotides in length. They fulfill essential regulatory functions by targeting the 3′ untranslated regions (3′-UTRs) of messenger RNAs (mRNAs) for cleavage or translational repression in a sequence-specific manner.[32] The miRNAs miR-143 and miR-145, categorized as intergenic, are located on chromosome 5 in humans and chromosome 18 in mice and rats. These miRNAs are notably expressed in vascular smooth muscle cells, within which the miR-143/145 cluster targets genes linked to phenotype transitions,[33] differentiation,[34,35] and interacts with ECs, ultimately influencing the stability of blood vessels.[36] Recently, Arderiu et al. discovered that a reduction in miR-145 expression facilitates the differentiation of adipocytes into ECs, thus enhancing angiogenesis.[37] Consequently, our hypothesis posits that miR-145 plays a pivotal role in the formation of microvascular structures and the differentiation of Sca1$^+$ progenitor cells into ECs. We discovered that miR-145-5p expression was significantly down-regulated during the differentiation process after VEGF treatment, while EC markers were up-regulated. Gain and loss-of-function experiments revealed that miR-145-5p plays a critical role in angiogenesis mediated by Sca1$^+$ progenitors, a finding that delineates a novel function of this microribonucleic acid. Previous studies had indicated that the miR-143/145 cluster modulates smooth muscle cell (SMC) differentiation and communication between SMCs and ECs.[38] The study by Arderiu et al. revealed that elevated miR-145 expression maintains the undifferentiated state of adipose-derived stem cells (ASCs). Conversely, reduction of miR-145 levels promotes EC differentiation from ASCs. Furthermore, miR-145 overexpression inhibits the migration of ASCs, and its knockdown enhances the expression of EC markers and the formation of capillary-like structures,[37] highly consistent with our results. Besides, it is also reported that miR-145 served as an inhibitory role in the angiogenesis in various tumors.[39,40] Other studies also showed that low serum level of miR-145 is associated with poor survival in cancer patients.[40,41] Therefore, given its role in angiogenesis, miR-145 is a potential diagnostic and prognostic marker for clinical applications.

Our findings also revealed ERG that acted as a downstream target of miR-145, which was particularly instrumental in the modulation of EC differentiation from Sca1$^+$ cells. In hematopoiesis[42] and angiogenesi,[43] ERG plays an important role as one of the Erythroblast transformation-specific transcription factors (ETS). CDH5 (VE-cadherin), an EC adhesion molecule, has been identified as a downstream target of the transcription factor ERG. Diminished ERG levels in human umbilical vein endothelial cells (HUVECs) precipitated cellular detachment and an augmented rate of apoptosis.[43] Consistently, our study revealed that enforced ERG overexpression enhances CDH5 expression.

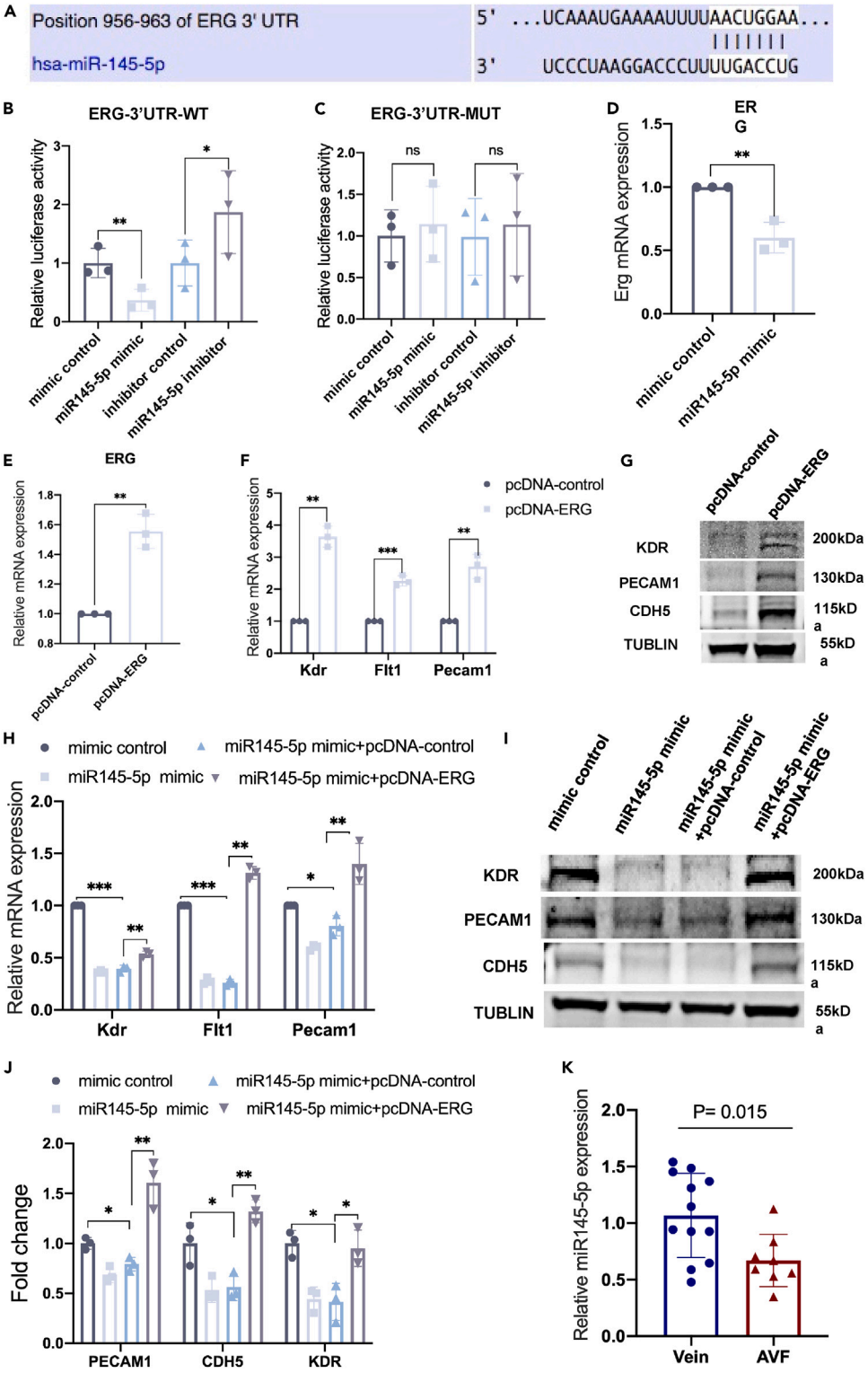

Figure 7. MiR-145-5p targets ERG to regulate differentiation of Sca1$^+$ cells into ECs

(A) The database TargetScan shows the combining site of miR-145-5p on ERG's 3′-UTR region.

(B) Luciferase activity of 293T cells co-transfected with wild type ERG-3′UTR and mimic control/miR-145-5p mimic or inhibitor control/miR-145-5p inhibitor.

(C) Luciferase activity of Sca1$^+$ cells co-transfected with mutant ERG-3′UTR and mimic control/miR-145-5p mimic or inhibitor control/miR-145-5p inhibitor.

(D) Erg mRNA expression in Sca1$^+$ cells transfected with mimic control or miR-145-5p mimic as measured by RT-PCR.

Figure 7. *Continued*

(E) ERG expression of Sca1$^+$ cells transfected with control plasmid vector (pcDNA-control) or plasmid to overexpress ERG (pcDNA-ERG) as measured by RT-PCR.
(F) mRNA expression of *Kdr*, *Pecam1* and *Flt1* in Sca1$^+$ cells transfected with pcDNA-control or pcDNA-ERG after treated with VEGF.
(G) Protein expression level of KDR, PECAM1, and CDH5 in Sca1$^+$ cells transfected with pcDNA-control or pcDNA-ERG after treated with VEGF.
(H) mRNA expression of *Kdr*, *Pecam1* and *Flt1* in Sca1$^+$ cells of each group as indicated.
(I) Protein expression level of KDR, PECAM1, and CDH5 in Sca1$^+$ cells of each group as indicated.
(J) Protein bands were quantified by densitometry and normalized to the density of Tubulin.
(K) Expression level of miR-145-5p in healthy cephalic vein and arteriovenous fistula (AVF) as determined by RT-PCR. *p* value between the 2 groups were specified in the graph. $n = 12$ in the healthy group and $n = 8$ in the AVF group. Data represent mean ± SEM. Statistical differences between groups were determined by one-way ANOVA analysis of variance with method of multiple comparisons or (D,E,K) two-tailed Student's *t* test for normally distributed values.*$p < 0.05$, **$p < 0.01$, ****$p < 0.0001$, ns $p \geq 0.05$. See also Figure S4-S7.

Furthermore, ERG modulates FLT1 (VEGFR1) expression[44,45] and a spectrum of additional genes pertinent to EC function.[46] Several previous studies have also corroborated the synergistic relationship between miR-145 and ERG.[47,48]

Conclusions

In summary, via scRNA-seq analyses, genetic lineage tracing and multiple mouse vessel surgery models, our study provided evidence that Sca1$^+$ vascular resident progenitor cells differentiated into ECs *in vitro* and *in vivo* under both arterial and venous remodeling. Mechanistically, we demonstrated that miR-145/ERG pathway was critical for this process. Inhibition of miR-145 locally markedly reduced neointimal hyperplasia in endothelial denudation models. The combined genetic and bioinformatic evidence of vascular Sca1$^+$ cells might provide insight into endothelial progenitors and contribute to a promising therapeutic approach for vascular diseases.

Limitations of the study

While our study demonstrated that Sca1$^+$ cells regenerate ECs *in vivo*, we have not conducted more studies on how they affect vascular pathology via more precise experiments such as Sca1-CreER^{T2};Rosa26-DTR mouse model, and ERG interfering methods. On the other hand, although we have proved that miR-145-5p/ERG pathway was a regulator in Sca1$^+$ cell's differentiation, in-depth studies on the downstream mechanism description will be needed. We will conduct further research on this signaling to elucidate how each individual signaling molecule affects Sca1$^+$ cell function, both in *in vitro* and *in vivo* studies.

STAR★METHODS

Detailed methods are provided in the online version of this paper and include the following:

- KEY RESOURCES TABLE
- RESOURCE AVAILABILITY
  - Lead contact
  - Materials availability
  - Data and code availability
- EXPERIMENTAL MODEL AND STUDY PARTICIPANT DETAILS
  - Ethics approval and consent to participate
  - Mouse experiment
  - Cell culture and transfection
- METHOD DETAILS
  - Femoral artery injury surgery
  - Veingraft surgery
  - Magnetic beads sorting
  - RNA isolation and reverse transcription (RT)-PCR assay
  - Western Blot
  - Immunofluorescence staining analyses
  - Assay for Dual-luciferase reporter genes
  - CCK8 proliferation assay
  - Transwell assay
  - Wound healing assay
  - Collection of human cephalic vein and fistula specimens
- QUANTIFICATION AND STATISTICAL ANALYSIS

SUPPLEMENTAL INFORMATION

Supplemental information can be found online at https://doi.org/10.1016/j.isci.2024.110080.

ACKNOWLEDGMENTS

We are grateful to Professor Qingbo Xu and Yanhua Hu for their help about the Sca1-CreER^{T2} knock-in mice. This work was supported by Alibaba-Zhejiang University Joint Research Center of Future Digital Healthcare and Alibaba Cloud. We are also grateful to the Core Facility Platform of Zhejiang University School of Medicine for technical assistance. We also thank the TargetScan database and GEO database database for the data. This work was supported by the grant from the National Key Research and Development Program of China (No. 2023YFC3606500), grants from the National Natural Science Foundation of China (No.82170489, 82200479); grants from the Natural Science Foundation of Zhejiang Province (No. LR22H020001, LY23H010007, LQ23H020005); a grant from the Project of Medical Science Research Foundation from the Health Department of Zhejiang Province (No. WKJ-ZJ-2312), and a grant from the Key Laboratory of Precision Medicine for Atherosclerotic Diseases of Zhejiang Province, China (No. 2022E10026). The funding bodies played no role in the design of the study and collection, analysis, and interpretation of data and in writing the manuscript.

AUTHOR CONTRIBUTIONS

T.C. and L.J. conceived ideas and designed the research. L.L., Z.Y., J.X., and X.X. performed mouse experiments and *in vitro* studies. Z.W. and M.C. analyzed scRNA-seq data. L.L., Z.L., Z.Y., L.J., and T.C. developed the figures and wrote the manuscript. Z.L. and T.C. obtained funding. All authors contributed to the manuscript.

DECLARATION OF INTERESTS

The authors declared no potential conflicts of interest.

Received: November 7, 2023
Revised: March 17, 2024
Accepted: May 20, 2024
Published: May 22, 2024

REFERENCES

1. Gomez-Salinero, J.M., and Rafii, S. (2018). Endothelial cell adaptation in regeneration. Science *362*, 1116–1117. https://doi.org/10.1126/science.aar4800.
2. Marcelo, K.L., Goldie, L.C., and Hirschi, K.K. (2013). Regulation of endothelial cell differentiation and specification. Circ. Res. *112*, 1272–1287. https://doi.org/10.1161/CIRCRESAHA.113.300506.
3. Su, W., Wang, L., Zhou, M., Liu, Z., Hu, S., Tong, L., Liu, Y., Fan, Y., Kong, D., Zheng, Y., et al. (2013). Human embryonic stem cell-derived endothelial cells as cellular delivery vehicles for treatment of metastatic breast cancer. Cell Transplant. *22*, 2079–2090. https://doi.org/10.3727/096368912X657927.
4. Wang, Z.Z., Au, P., Chen, T., Shao, Y., Daheron, L.M., Bai, H., Arzigian, M., Fukumura, D., Jain, R.K., and Scadden, D.T. (2007). Endothelial cells derived from human embryonic stem cells form durable blood vessels in vivo. Nat. Biotechnol. *25*, 317–318. https://doi.org/10.1038/nbt1287.
5. Choi, K.D., Yu, J., Smuga-Otto, K., Salvagiotto, G., Rehrauer, W., Vodyanik, M., Thomson, J., and Slukvin, I. (2009). Hematopoietic and endothelial differentiation of human induced pluripotent stem cells. Stem Cell. *27*, 559–567. https://doi.org/10.1634/stemcells.2008-0922.
6. Adams, W.J., Zhang, Y., Cloutier, J., Kuchimanchi, P., Newton, G., Sehrawat, S., Aird, W.C., Mayadas, T.N., Luscinskas, F.W., and García-Cardeña, G. (2013). Functional vascular endothelium derived from human induced pluripotent stem cells. Stem Cell Rep. *1*, 105–113. https://doi.org/10.1016/j.stemcr.2013.06.007.
7. Chatterjee, I., Li, F., Kohler, E.E., Rehman, J., Malik, A.B., and Wary, K.K. (2016). Induced Pluripotent Stem (iPS) Cell Culture Methods and Induction of Differentiation into Endothelial Cells. Methods Mol. Biol. *1357*, 311–327. https://doi.org/10.1007/7651_2015_203.
8. Krenning, G., Strate, B.W.A.v.d., Schipper, M., van Seijen, X.J.G.Y., Fernandes, B.C.A., van Luyn, M.J.A., and Harmsen, M.C. (2009). CD34+ cells augment endothelial cell differentiation of CD14+ endothelial progenitor cells in vitro. J. Cell Mol. Med. *13*, 2521–2533. https://doi.org/10.1111/j.1582-4934.2008.00479.x.
9. Jang, J.H., Kim, S.K., Choi, J.E., Kim, Y.J., Lee, H.W., Kang, S.Y., Park, J.S., Choi, J.H., Lim, H.Y., and Kim, H.C. (2007). Endothelial progenitor cell differentiation using cryopreserved, umbilical cord blood-derived mononuclear cells. Acta Pharmacol. Sin. *28*, 367–374. https://doi.org/10.1111/j.1745-7254.2007.00519.x.
10. Margariti, A., Winkler, B., Karamariti, E., Zampetaki, A., Tsai, T.N., Baban, D., Ragoussis, J., Huang, Y., Han, J.D.J., Zeng, L., et al. (2012). Direct reprogramming of fibroblasts into endothelial cells capable of angiogenesis and reendothelialization in tissue-engineered vessels. Proc. Natl. Acad. Sci. USA *109*, 13793–13798. https://doi.org/10.1073/pnas.1205526109.
11. Jiang, L., Chen, T., Sun, S., Wang, R., Deng, J., Lyu, L., Wu, H., Yang, M., Pu, X., Du, L., et al. (2021). Nonbone Marrow CD34(+) Cells Are Crucial for Endothelial Repair of Injured Artery. Circ. Res. *129*, e146–e165. https://doi.org/10.1161/CIRCRESAHA.121.319494.
12. Le Bras, A., Yu, B., Issa Bhaloo, S., Hong, X., Zhang, Z., Hu, Y., and Xu, Q. (2018). Adventitial Sca1+ Cells Transduced With ETV2 Are Committed to the Endothelial Fate and Improve Vascular Remodeling After Injury. Arterioscler. Thromb. Vasc. Biol. *38*, 232–244. https://doi.org/10.1161/ATVBAHA.117.309853.
13. Ren, X., Ustiyan, V., Guo, M., Wang, G., Bolte, C., Zhang, Y., Xu, Y., Whitsett, J.A., Kalin, T.V., and Kalinichenko, V.V. (2019). Postnatal Alveologenesis Depends on FOXF1 Signaling in c-KIT(+) Endothelial Progenitor Cells. Am. J. Respir. Crit. Care Med. *200*, 1164–1176. https://doi.org/10.1164/rccm.201812-2312OC.
14. Kattman, S.J., Huber, T.L., and Keller, G.M. (2006). Multipotent flk-1+ cardiovascular progenitor cells give rise to the cardiomyocyte, endothelial, and vascular smooth muscle lineages. Dev. Cell *11*, 723–732. https://doi.org/10.1016/j.devcel.2006.10.002.
15. van de Rijn, M., Heimfeld, S., Spangrude, G.J., and Weissman, I.L. (1989). Mouse hematopoietic stem-cell antigen Sca-1 is a member of the Ly-6 antigen family. Proc. Natl. Acad. Sci. USA *86*, 4634–4638. https://doi.org/10.1073/pnas.86.12.4634.
16. Tang, J., Zhu, H., Liu, S., Wang, H., Huang, X., Yan, Y., Wang, L., and Zhou, B. (2021). Sca1 marks a reserve endothelial progenitor population that preferentially expand after injury. Cell Discov. *7*, 88. https://doi.org/10.1038/s41421-021-00303-z.
17. Beltrami, A.P., Barlucchi, L., Torella, D., Baker, M., Limana, F., Chimenti, S., Kasahara, H., Rota, M., Musso, E., Urbanek, K., et al. (2003). Adult cardiac stem cells are multipotent and support myocardial regeneration. Cell *114*, 763–776. https://doi.org/10.1016/s0092-8674(03)00687-1.
18. Small, E.M., Frost, R.J.A., and Olson, E.N. (2010). MicroRNAs add a new dimension to cardiovascular disease. Circulation *121*, 1022–1032. https://doi.org/10.1161/CIRCULATIONAHA.109.889048.
19. Hall, I.F., Climent, M., Quintavalle, M., Farina, F.M., Schorn, T., Zani, S., Carullo, P., Kunderfranco, P., Civilini, E., Condorelli, G.,

and Elia, L. (2019). Circ_Lrp6, a Circular RNA Enriched in Vascular Smooth Muscle Cells, Acts as a Sponge Regulating miRNA-145 Function. Circ. Res. *124*, 498–510. https://doi.org/10.1161/CIRCRESAHA.118.314240.

20. Baltzinger, M., Mager-Heckel, A.M., and Remy, P. (1999). Xl erg: expression pattern and overexpression during development plead for a role in endothelial cell differentiation. Dev. Dyn. *216*, 420–433. https://doi.org/10.1002/(SICI)1097-0177(199912)216:4/5<420::AID-DVDY10>3.0.CO;2-C.
21. Ross, R. (1986). The pathogenesis of atherosclerosis–an update. N. Engl. J. Med. *314*, 488–500. https://doi.org/10.1056/NEJM198602203140806.
22. Asahara, T., Murohara, T., Sullivan, A., Silver, M., van der Zee, R., Li, T., Witzenbichler, B., Schatteman, G., and Isner, J.M. (1997). Isolation of Putative Progenitor Endothelial Cells for Angiogenesis. Science *275*, 964–967. https://doi.org/10.1126/science.275.5302.964.
23. Schachinger, V., Erbs, S., Elsasser, A., Haberbosch, W., Hambrecht, R., Holschermann, H., Yu, J., Corti, R., Mathey, D.G., Hamm, C.W., et al. (2006). Improved clinical outcome after intracoronary administration of bone-marrow-derived progenitor cells in acute myocardial infarction: final 1-year results of the REPAIR-AMI trial. Eur. Heart J. *27*, 2775–2783. https://doi.org/10.1093/eurheartj/ehl388.
24. Surder, D., Manka, R., Moccetti, T., Lo Cicero, V., Emmert, M.Y., Klersy, C., Soncin, S., Turchetto, L., Radrizzani, M., Zuber, M., et al. (2016). Effect of Bone Marrow-Derived Mononuclear Cell Treatment, Early or Late After Acute Myocardial Infarction: Twelve Months CMR and Long-Term Clinical Results. Circ. Res. *119*, 481–490. https://doi.org/10.1161/CIRCRESAHA.116.308639.
25. Marvasti, T.B., Alibhai, F.J., Weisel, R.D., and Li, R.-K. (2019). CD34+ Stem Cells: Promising Roles in Cardiac Repair and Regeneration. Can. J. Cardiol. *35*, 1311–1321. https://doi.org/10.1016/j.cjca.2019.05.037.
26. Hu, Y., Zhang, Z., Torsney, E., Afzal, A.R., Davison, F., Metzler, B., and Xu, Q. (2004). Abundant progenitor cells in the adventitia contribute to atherosclerosis of vein grafts in ApoE-deficient mice. J. Clin. Invest. *113*, 1258–1265. https://doi.org/10.1172/jci19628.
27. Ingram, D.A., Mead, L.E., Moore, D.B., Woodard, W., Fenoglio, A., and Yoder, M.C. (2005). Vessel wall–derived endothelial cells rapidly proliferate because they contain a complete hierarchy of endothelial progenitor cells. Blood *105*, 2783–2786. https://doi.org/10.1182/blood-2004-08-3057.
28. Zengin, E., Chalajour, F., Gehling, U.M., Ito, W.D., Treede, H., Lauke, H., Weil, J., Reichenspurner, H., Kilic, N., and Ergün, S. (2006). Vascular wall resident progenitor cells: a source for postnatal vasculogenesis. Development *133*, 1543–1551. https://doi.org/10.1242/dev.02315.
29. Qu-Petersen, Z., Deasy, B., Jankowski, R., Ikezawa, M., Cummins, J., Pruchnic, R., Mytinger, J., Cao, B., Gates, C., Wernig, A., and Huard, J. (2002). Identification of a novel population of muscle stem cells in mice: potential for muscle regeneration. J. Cell Biol. *157*, 851–864. https://doi.org/10.1083/jcb.200108150.
30. Oh, H., Bradfute, S.B., Gallardo, T.D., Nakamura, T., Gaussin, V., Mishina, Y., Pocius, J., Michael, L.H., Behringer, R.R., Garry, D.J., et al. (2003). Cardiac progenitor cells from adult myocardium: homing, differentiation, and fusion after infarction. Proc. Natl. Acad. Sci. USA *100*, 12313–12318. https://doi.org/10.1073/pnas.2132126100.
31. Pfister, O., Mouquet, F., Jain, M., Summer, R., Helmes, M., Fine, A., Colucci, W.S., and Liao, R. (2005). CD31- but Not CD31+ cardiac side population cells exhibit functional cardiomyogenic differentiation. Circ. Res. *97*, 52–61. https://doi.org/10.1161/01.RES.0000173297.53793.fa.
32. Bartel, D.P. (2004). MicroRNAs: genomics, biogenesis, mechanism, and function. Cell *116*, 281–297. https://doi.org/10.1016/s0092-8674(04)00045-5.
33. Boettger, T., Beetz, N., Kostin, S., Schneider, J., Krüger, M., Hein, L., and Braun, T. (2009). Acquisition of the contractile phenotype by murine arterial smooth muscle cells depends on the Mir143/145 gene cluster. J. Clin. Invest. *119*, 2634–2647. https://doi.org/10.1172/JCI38864.
34. Cordes, K.R., Sheehy, N.T., White, M.P., Berry, E.C., Morton, S.U., Muth, A.N., Lee, T.H., Miano, J.M., Ivey, K.N., and Srivastava, D. (2009). miR-145 and miR-143 regulate smooth muscle cell fate and plasticity. Nature *460*, 705–710. https://doi.org/10.1038/nature08195.
35. Elia, L., Quintavalle, M., Zhang, J., Contu, R., Cossu, L., Latronico, M.V.G., Peterson, K.L., Indolfi, C., Catalucci, D., Chen, J., et al. (2009). The knockout of miR-143 and -145 alters smooth muscle cell maintenance and vascular homeostasis in mice: correlates with human disease. Cell Death Differ. *16*, 1590–1598. https://doi.org/10.1038/cdd.2009.153.
36. Climent, M., Quintavalle, M., Miragoli, M., Chen, J., Condorelli, G., and Elia, L. (2015). TGFβ Triggers miR-143/145 Transfer From Smooth Muscle Cells to Endothelial Cells, Thereby Modulating Vessel Stabilization. Circ. Res. *116*, 1753–1764. https://doi.org/10.1161/CIRCRESAHA.116.305178.
37. Arderiu, G., Peña, E., Aledo, R., Juan-Babot, O., Crespo, J., Vilahur, G., Oñate, B., Moscatiello, F., and Badimon, L. (2019). MicroRNA-145 Regulates the Differentiation of Adipose Stem Cells Toward Microvascular Endothelial Cells and Promotes Angiogenesis. Circ. Res. *125*, 74–89. https://doi.org/10.1161/CIRCRESAHA.118.314290.
38. Deng, L., Blanco, F.J., Stevens, H., Lu, R., Caudrillier, A., McBride, M., McClure, J.D., Grant, J., Thomas, M., Frid, M., et al. (2015). MicroRNA-143 Activation Regulates Smooth Muscle and Endothelial Cell Crosstalk in Pulmonary Arterial Hypertension. Circ. Res. *117*, 870–883. https://doi.org/10.1161/CIRCRESAHA.115.306806.
39. Xu, W., Chang, J., Du, X., and Hou, J. (2017). Long non-coding RNA PCAT-1 contributes to tumorigenesis by regulating FSCN1 via miR-145-5p in prostate cancer. Biomed. Pharmacother. *95*, 1112–1118. https://doi.org/10.1016/j.biopha.2017.09.019.
40. Zhang, Y., Wen, X., Hu, X.L., Cheng, L.Z., Yu, J.Y., and Wei, Z.B. (2016). Downregulation of miR-145-5p correlates with poor prognosis in gastric cancer. Eur. Rev. Med. Pharmacol. Sci. *20*, 3026–3030.
41. Geater, S.L., Chaniad, P., Trakunram, K., Keeratichananont, W., Buya, S., Thongsuksai, P., and Raungrut, P. (2022). Diagnostic and prognostic value of serum miR-145 and vascular endothelial growth factor in non-small cell lung cancer. Oncol. Lett. *23*, 12. https://doi.org/10.3892/ol.2021.13130.
42. Loughran, S.J., Kruse, E.A., Hacking, D.F., de Graaf, C.A., Hyland, C.D., Willson, T.A., Henley, K.J., Ellis, S., Voss, A.K., Metcalf, D., et al. (2008). The transcription factor Erg is essential for definitive hematopoiesis and the function of adult hematopoietic stem cells. Nat. Immunol. *9*, 810–819. https://doi.org/10.1038/ni.1617.
43. Birdsey, G.M., Dryden, N.H., Amsellem, V., Gebhardt, F., Sahnan, K., Haskard, D.O., Dejana, E., Mason, J.C., and Randi, A.M. (2008). Transcription factor Erg regulates angiogenesis and endothelial apoptosis through VE-cadherin. Blood *111*, 3498–3506. https://doi.org/10.1182/blood-2007-08-105346.
44. Tsourlakis, M.C., Khosrawi, P., Weigand, P., Kluth, M., Hube-Magg, C., Minner, S., Koop, C., Graefen, M., Heinzer, H., Wittmer, C., et al. (2015). VEGFR-1 overexpression identifies a small subgroup of aggressive prostate cancers in patients treated by prostatectomy. Int. J. Mol. Sci. *16*, 8591–8606. https://doi.org/10.3390/ijms16048591.
45. Valter, M.M., Hügel, A., Huang, H.J., Cavenee, W.K., Wiestler, O.D., Pietsch, T., and Wernert, N. (1999). Expression of the Ets-1 transcription factor in human astrocytomas is associated with Fms-like tyrosine kinase-1 (Flt-1)/vascular endothelial growth factor receptor-1 synthesis and neoangiogenesis. Cancer Res. *59*, 5608–5614.
46. Lelievre, E., Lionneton, F., Soncin, F., and Vandenbunder, B. (2001). The Ets family contains transcriptional activators and repressors involved in angiogenesis. Int. J. Biochem. Cell Biol. *33*, 391–407. https://doi.org/10.1016/s1357-2725(01)00025-5.
47. Li, S., Wu, X., Xu, Y., Wu, S., Li, Z., Chen, R., Huang, N., Zhu, Z., and Xu, X. (2016). miR-145 suppresses colorectal cancer cell migration and invasion by targeting an ETS-related gene. Oncol. Rep. *36*, 1917–1926. https://doi.org/10.3892/or.2016.5042.
48. Hart, M., Wach, S., Nolte, E., Szczyrba, J., Menon, R., Taubert, H., Hartmann, A., Stoehr, R., Wieland, W., Grässer, F.A., and Wullich, B. (2013). The proto-oncogene ERG is a target of microRNA miR-145 in prostate cancer. FEBS J. *280*, 2105–2116. https://doi.org/10.1111/febs.12236.
49. Ni, Z., Lyu, L., Gong, H., Du, L., Wen, Z., Jiang, H., Yang, H., Hu, Y., Zhang, B., Xu, Q., et al. (2023). Multilineage commitment of Sca-1^{+} cells in reshaping vein grafts. Theranostics *13*, 2154–2175. https://doi.org/10.7150/thno.77735.
50. Lyu, L., Li, Z., Wen, Z., He, Y., Wang, X., Jiang, L., Zhou, X., Huang, C., Wu, Y., Chen, T., and Guo, X. (2023). Fate mapping RNA-sequencing reveal Malat1 regulates Sca1+ progenitor cells to vascular smooth muscle cells transition in vascular remodeling. Cell. Mol. Life Sci. *80*, 118. https://doi.org/10.1007/s00018-023-04762-3.

STAR★METHODS

KEY RESOURCES TABLE

REAGENT or RESOURCE	SOURCE	IDENTIFIER
Antibodies		
Goat polyclonal anti-CD31 Antibody	R&D Systems	Cat#AF3628; RRID:AB_2161028
Rabbit Polyclonal RFP Antibody	Rockland	Cat#600-401-379; RRID:AB_2209751
Anti-CDH5 antibody	Abcam	Cat#ab33168; RRID:AB_870662
Recombinant Anti-VEGF Receptor 2 antibody	Abcam	Cat# ab134191; RRID:AB_2934135
Rabbit polyclonal ERG antibody	Proteintech	Cat#14356-1-AP; RRID:AB_2098423
Donkey anti-rabbit IgG Alexa Fluor 555	Invitrogen	Cat# A31572; RRID: AB_162543
Donkey anti-goat IgG Alexa Fluor 488	Invitrogen	Cat# A11055; RRID: AB_2534102
Rat Monoclonal anti-Sca1 Antibody	Abcam	Cat#ab51317; RRID:AB_1640946
HRP-labeled Goat Anti-Rabbit IgG(H + L)	Beyotime	Cat# A0208; RRID:AB_2892644
Donkey anti-mouse IgG (H + L)	Invitrogen	Cat# A-21203; RRID: AB_141633
Biological samples		
Human cephalic vein and fistula specimens	Zhejiang University's First Affiliated Hospital	N/A
Chemicals, peptides, and recombinant proteins		
EGM-2 medium	Lonza	Cat# CC-3162
VEGF	PeproTech	Cat# AF-450-32-10
CCK8	Dojindo	Cat# CK04
Transwell chamber	Corning	Cat#3460
LIF	Merck	Cat# LIF1050
Penicillin	Cienry	Cat# CR- 15140
Streptomycin	Cienry	Cat# CR- 15140
β-ME	Sigma	Cat# M3148
Tamoxifen	Sigma	Cat# C8267
DMEM	ATCC	Cat# 30-2002
Fetal bovine serum	Embriomax	Cat# ES-009-B
Opti-MEM	Gibco	Cat# 31985-070
RNAiMAX	Invitrogen	Cat# 13778150
Lipo3000	Invitrogen	Cat# L3000015
Prime Script RT master mix	Takara	Cat#RR036A
SYBR Premix Ex Taq	Takara	Cat# RR820A
RIPA Lysis Buffer	Solarbio	Cat# R0010
Critical commercial assays		
Sca1+ microbeads kit	Miltenyi Biotec	Cat#130-122-615
RNA Purification Kit	EZBioscience	Cat#B0004D
Luciferase reporter assay kit	Promega	Cat# PR-E1910
Cell counting kit-8	Dojindo	Cat# CK04
Deposited data		

(*Continued on next page*)

Continued

REAGENT or RESOURCE	SOURCE	IDENTIFIER
RNA-sequencing data	GEO	GEO:GSE182232
Experimental models: Cell lines		
Mouse aortic endothelial cell line	Procell	Cat# CP-M075
Experimental models: Organisms/strains		
Sca1-CreERT2 mice (C57BL/6)	Shanghai Model Organisms Center,Inc.	N/A
Rosa26-tdTomato mice (C57BL/6)	Shanghai Model Organisms Center,Inc.	N/A
Rosa26-iDTR mice (C57BL/6)	Shanghai Model Organisms Center,Inc.	N/A
C57BL/6 wild-type mice	Shanghai Slack Laboratory Animal Co. LTD	N/A
Oligonucleotides		
miR145-5p mimic sense: 5′-GUCCAGUUUUCCCAGGAAUCCCU-3′	GenePharma	N/A
miR145-5p inhibitor: 5′-AGGGAUUCCUGGGAAAACUGGAC-3′	GenePharma	N/A
Primers for qPCR, see Table S1	GenePharma	N/A
miR145-5p antagomir, see Table S1	RiboBio	N/A
Recombinant DNA		
plasmids (pcDNA-ERG), see Table S1	Hanbio	N/A
Dual luciferase reporter gene plasmid, see Table S1	GenePharma	N/A
Software and algorithms		
CellRanger(v3.1.0).	10x Genomics	https://www.10xgenomics.com/support/software/cell-ranger/downloads
RStudio (v3.6)	RStudio	https://rstudio.com/products/rstudio/download/
R(v4.2.3)	The R project	https://www.r-project.org/
GraphPad Prism 9	GraphPad Software	https://www.graphpad.com/
Seurat (v3.2.3)	Satija Lab	https://satijalab.org/seurat/articles/install.html
Monocle (v2.8.0)	Trapnell Lab	https://cole-trapnell-lab.github.io/monocle-release/
Fiji	NIH	https://imagej.net/software/fiji/downloads

RESOURCE AVAILABILITY

Lead contact

Further information and requests for resources should be directed to and will be fulfilled by the lead contact, Ting Chen (ct010151452@zju.edu.cn).

Materials availability

This study did not generate any new materials.

Data and code availability

- The scRNA-seq data used in this study was a public dataset that had been deposited in the NCBI Gene Expression Omnibus and are accessible through the GEO Series accession number GSE182232.
- This paper does not report original code.
- Any additional information required to reanalyze the data reported in this paper is available from the lead contact upon request.

EXPERIMENTAL MODEL AND STUDY PARTICIPANT DETAILS

Ethics approval and consent to participate

All animal experiments and protocols were performed in accordance with the National Institutes of Health's Guide for the Care and Use of Laboratory. The animal studies were approved by the Research Ethics Committees of the First Affiliated Hospital of Zhejiang University (Title,

The role of Sca1positive cells and the mechanism in vascular remodeling; The Tab of Animal Experimental Ethical Inspection of the First Affiliated Hospital, Zhejiang University School of Medicine; Approval Reference No. 2021/159; Date, February 4, 2021). All animal experiments were conducted according to the ARRIVE guidelines. As for the human vascular samples, the study protocol was approved by the Research Ethics Committees of the First Affiliated Hospital of Zhejiang University (Title, Stem cells in cardiovascular diseases and exploring novel mechanisms; Clinical Research Ethics Committees of the First Affiliated Hospital, College of medicine, Zhejiang; Approval Reference No. 2021/330; Date, May 10, 2021), and written informed consent was obtained from all patients, which clearly stated the purpose of our study.

Mouse experiment

Animal experiments were performed in accordance with the US National Institutes of Health's Guide for Care and Use of Laboratory Animals (8th edition, 2011) and the committee of Zhejiang University School of Medicine approved the animal care and use experiments. Mice were housed in a temperature and humidity-controlled barrier facility on a 12-hour light-dark schedule and fed *ad libitum* with standard rodent chow.

To generate Sca1-CreER^{T2};Rosa26-tdTomato mice, Sca1-CreER^{T2} mice obtained from Shanghai Model Organisms Centers, Inc. bred with Rosa26-tdTomato mice from Shanghai Slack Laboratory Animal Co. LTD.

For femoral artery guidewire injury surgery, 8-12-week-old Sca1-CreER^{T2}; Rosa26-tdTomato male and female mice were randomly divided into different experimental groups. To activate tdTomato labeling on Sca1^{+} cells, a diluted solution of tamoxifen was administered by gavage to mice (0.1-0.15 mg/gram body weight) in corn oil (20 mg/mL). After that, in accordance with the previous description, the surgery for guide wire injury was done one week later.[11]

To investigate the role of miR-145-5p *in vivo*, Sca1-CreER^{T2}; Rosa26-tdTomato male and female mice were fed a tamoxifen diet for 2 weeks and randomly divided into 2 groups before femoral artery injury surgery. After wire injury, 100 μl of 30% pluronic gel containing 2.5 nmol miR-145-5p antagomir or antago-control was applied perivascularly to injured femoral arteries. After 4 weeks, the samples were harvested and immunofluorescence staining was performed. Sequence of miR145-5p antagomir used *in vivo* was described in Table S1.

For veingraft surgeries, wild-type vena cava were transplanted into Sca1-CreER^{T2};Rosa26-tdTomato mice's carotid arteries as previously described.[49]

Cell culture and transfection

Cells isolated from the aortic arch of C57 wild-type mice were then sorted with Sca1 (Miltenyi Biotec, 130-122-615) microbeads according to manufacturer's instructions. The sorted Sca1^{+} cells were then cultured in cell culture medium and passed every 3 days at a ratio of 1:3. This cell culture medium contains DMEM (ATCC, 30-2002) supplemented by 10% fetal bovine serum (Embriomax, ES-009-B), 10ng/ml leukemia inhibitory factor (Merck Millipore, LIF1050), and 0.1 mM 2-mercaptoethanol (Sigma, M3148) and a mixture of 100 U/mL Penicillin-Streptomycin solution (Cienry, CR-15140).

For endothelial differentiation from Sca1^{+} cells, the cells were cultured in Endothelial Cell Growth Medium-2 (Lonza, CC-3162) supplemented with 50ng/ml VEGF (PeproTech, 96-450-32-10). Five days later, the cells were stained for Sca1 and CD31.

For microRNA mimic and inhibitor transfection, the culture medium was replaced with Opti-MEM (Gibco, 31985-070) for 12 hours to starve the Sca1^{+} cells. And mimics/inhibitors were transfected with RNAiMAX (Invitrogen, 13778150). A DNA transfection reagent (Lipo3000, L3000015) was used to transfect plasmids (pcDNA-ERG) that overexpress ERG. Sequences used for cell transfection were listed in Table S1.

METHOD DETAILS

Femoral artery injury surgery

After anesthesia, the mice were fixed in the supine position, and the surgical area was depilated and sterilized. The inguinal incision was made under a stereomicroscope, and the saphenous artery was isolated. Arteriotomy was performed with a 30 G insulin needle tip (diameter 0.31 mm), and then a 0.25 mm tip guidewire (Abbott Cross-IT 200XT guidewire tip) was inserted. After the guide wire was inserted into the saphenous artery, it was pushed forward into the femoral artery until it entered the iliac artery. The guide wire was pushed back and forth from multiple angles for 10 times, and then it was left for 3 minutes to dilate the artery and strip the intima. After 3 minutes, the guide wire was withdrawn, the saphenous artery was ligated, blood flow was restored, and the skin was sutured.

Veingraft surgery

The vena cava was extracted from donor mice and preserved in a saline solution containing heparin (100 U/mL). The recipient mouse was anesthetized with phenobarbital sodium (50 mg/kg) via intraperitoneal injection. A midline incision was made in the neck of the recipient mouse, followed by careful isolation and exposure of the right common carotid artery. Both ends of the artery were securely clipped after dissection, and a 1 mm diameter cuff was placed over each end. The vena cava harvested from donor mice was surgically grafted between the two ends of the artery. Each end of the vena cava was securely fastened around the carotid artery and ligated with an 8-0 suture. Following the careful removal of the artery clippers, the presence of vigorous pulsation in the vein confirmed a successful engraftment.

Magnetic beads sorting

The cells were washed once with binding buffer. After digestion and centrifugation, the cells were resuspended by adding appropriate Sca1-FITC antibody (Miltenyi,130-092-529), and incubated at 4°C for 15 min, while shaken every 3min.Cells were resuspended by adding a 10-fold volume of binding buffer, followed by centrifugation (400g, 8min, 4°C), then resuspended with appropriate amount of anti-FITC immunomagnetic beads (Miltenyi, 130-048-701), incubated at 4°C for 15 minutes, and shaken upside down every 3min. Cells were resuspended by adding a 10-fold volume of binding buffer, followed by centrifugation (400g, 8min, 4°C). Cells were then resuspended with the appropriate amount of binding buffer. The magnetic frame and separation column were prepared and pre-washed with binding buffer, followed by column passing. The separation column was placed inside the centrifuge tube, an appropriate amount of binding buffer was added to the separation column, and the bound $Sca1^+$ cells on the column were forcefully flushed out with a piston.

RNA isolation and reverse transcription (RT)-PCR assay

Total RNA was extracted from the samples using from the EZ-press RNA Purification Kit (EZBioscience, B0004D) and reverse transcribed into first-strand cDNA using a Prime Script RT master mix (Takara, RR036A). The final quantitative real-time PCR reaction mix contained 5μL SYBR Premix Ex Taq (TaKaRa, RR820A), 1 μl cDNA, 1 μl primers, and 3 μl DEPC water. Amplification was performed on Quantstudio5DX (Thermo, USA). The relative expression levels were detected and analyzed based on the formula of $2-\Delta\Delta ct$. Primers for RT-PCR were listed in Table S1.

Western Blot

A RIPA Lysis Buffer (Solarbio, R0010) was used to lyse cells for 40 minutes at 4°C followed by 10 minutes of loading dye investigation. The protein concentration was measured by BCA method. Proteins were separated by SDS-PAGE and transferred to PVDF, blocked with bovine serum albumin for 1h, and then incubated with primary antibodies in blocking buffer overnight at 4°C. After washing with TBST, secondary antibodies were added and incubated at room temperature for 5min. ECL luminescence solution and imaging instrument were used to expose the image.

Immunofluorescence staining analyses

For femoral artery and veingraft samples, tissue was harvested at the indicated time points, rinsed in 4% paraformaldehyde, dehydrated in 30% sucrose solution, embedded in OCT at -80°C and sliced into 8-μm thick sections. For cultured cells, paraformaldehyde was applied for 15 minutes to fix the cells. Subsequent immunofluorescence staining was performed as previously described.[11] Antibodies used in this study were listed in the key resources table. A Nikon A1 Ti confocal microscope and an Olympus FV3000 confocal microscope were used to acquire cryosection and cell staining images, further analyzed by relevant software. Regions were selected randomly to avoid biasing.

Assay for Dual-luciferase reporter genes

Full 3′UTR (WT-3′UTR) or mutant 3′UTR (mut-3′UTR) of ERG was cloned into the luciferase reporter based on the GP-miRGLO vector. A luciferase reporter plasmid was co-transfected with either control/miR-145-5p mimics or control/miR-145-5p inhibitors by using RNAiMAX and Neofect together. Six hours after transfection, the medium was changed. 20μl of cell lysate buffer was added to each well of a 96-well plate and the plates were shaken for 15min at room temperature. To each well of a 96-well plate, 20μl of cell lysates and 100μl of fluorin working solution (1X) were added, and the fluorescence value of firefly luciferase was measured in a microplate reader. After that, 100μl of termination solution was quickly added and the renilla luciferase fluorescence value was measured. Relative luciferase activity was defined as the ratio of luciferase activity to renilla activity. The control was set at 1.0.

CCK8 proliferation assay

CCK8 assay was performed using the cell counting kit-8 (Dojindo, CK04). After transfections with mimic control or miR-145-5p mimic, $Sca1^+$ SPCs were cultured in a complete stem cell medium for 12 hours. Then, cells were trypsinized and seeded into a gelatin-coated 96-well plate (5000 cells/200 μl/well). After incubating for 1, 2, 3 days, the medium was replaced with 10 μl CCK8 solution supplemented with 90 μl DMEM. The OD was measured at 450 nm after incubating for 1 h at 37°C.

Transwell assay

Cells were transfected and treated as described in the CCK8 assay. Cell suspension aliquots (20,000 cells/500μl) were seeded in the upper chamber of a transwell insert (Corning, 3422). Additionally, mouse aortic endothelial cells and 1000 μl of EGM-2 containing 2% FBS was added to the lower chamber, then incubated at 37°C and 5% CO_2 for 12∼18 h. Following that, the inserts were fixed with 4% paraformaldehyde for 30 minutes and stained with 0.1% crystal violet for 30 minutes. Cotton swabs were used to wipe off non-migrated cells on the upper side of the insert after washing. The cells remaining under the membrane were the migrated ones and were assessed by a Zeiss microscope (20x magnification).

Wound healing assay

Cells were seeded into a 6-well plate pre-coated with 0.1% gelatin. After adherence, the wounds were created using 1000μl pipette tips, and images were taken at given intervals, including 0 h, 12, and 24 hours under a microscope. The percentage of wound closure was calculated by measuring the cell-free area at different times with ImageJ.

Collection of human cephalic vein and fistula specimens

The collection of human cephalic vein and fistula specimens were described as previously.[50] Zhejiang University's First Affiliated Hospital's Research Ethics Committee reviewed and approved studies that involved human subjects (Institutional Review Board Approval No. 2021/330). A collection of normal cephalic vein samples was taken from 12 patients who received their first arteriovenostomy. The arteriovenous fistula (AVF) samples were obtained from 8 patients who underwent AVF ligation after kidney transplants.

QUANTIFICATION AND STATISTICAL ANALYSIS

All data are presented as mean ± standard error of the mean (SEM). The number of animals or repeats used in the study is shown in each figure legend. GraphPad including a statistical package is used for conducting statistical analyses. Statistical differences among multiple groups were determined by one-way ANOVA analyses, whlile data from two groups were analyzed by two-tailed Student's t test. $P < 0.05$ is considered significant.